To provide our experiments with solid foundation, we incorporated theoretical analysis into the entire construction, verification and application of SPOT. Considering the basic feature of SPOT is the spontaneous formation of granules, we first computed the approximate phase diagrams concerning the conditions for phase separation from a thermodynamic perspective. For a more dynamic process, we also simulated liquid-liquid phase separation based on stochastic Cahn-Hilliard equation. The partial differential equations are solved by finite-element method under Neumann boundary condition, along with Crank-Nicolson scheme for time stepping. We altered an parameter named χ to predict what will happen if we change the strength of interaction, presumably the concentration of inducer.

Based on the simulation of phase separation, we explored the potential applications of SPOT, for instance, metabolic regulation. In this case, previously simulated separation process can represent the concentration of enzymes in a temporal sequence. We coupled it with a typical enzyme kinetic reaction to predict how would SPOT affect reaction rate.

SIMULATION FOR PHASE SEPARATION

Considering that our project is mainly predicated on liquid-liquid phase separation, we simulated phase separation of a ternary mixture in silico for deeper understanding and approximate predictions of our experiments. To better demonstrate the underlying principles, we started with a binary mixture to see why and when two components s will separate.

Generally, when intermolecular interactions are neglected (i.e. all molecules can be treated independently), two components tend to mix with each other until entropy reaches its maximum. The resulting homogeneous mixed state remains stable in this case. For instance, water and ethanol can be mixed at any ratio.

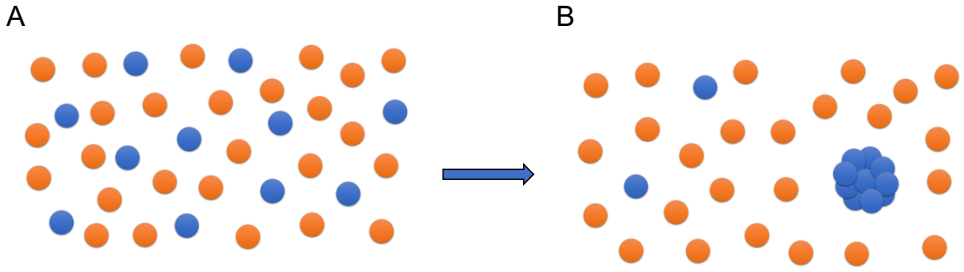

Figure. 1: (A) Mixed binary mixture, circles with different colors denote different molecules. (B) Demixed binary mixture, one component forms a dense liquid droplet

Things might get a little different when interaction among molecules are considered. Under the conditions of constant temperature, volume and particle numbers, the system is at equilibrium when the **Helmholtz free energy** F is the lowest. Based on regular solution model, the free energy density f takes the following form in the unit of k_BT [1]:

$$f = \phi \ln \phi + (1-\phi)\ln(1-\phi) + +\chi\phi(1-\phi) + \frac{\lambda}{2}|\nabla\phi|^2, \qquad (1)$$

where ϕ is the volume fraction of one component (let us say component A), χ is a parameter characterizing the strength of intermolecular interactions, and λ is related to the surface tension between interfaces. The volume fraction of A is defined as the volume of A molecules divided by the total volume of the system. In a binary system, the volume fraction of the other component, let us say component B, naturally becomes $1-\phi$.

First let's focus on the symmetric part of f , i.e $f_0 = \phi \ln \phi + (1-\phi)\ln(1-\phi) + \chi\phi(1-\phi)$, and see how its shape changes as we vary χ. When A and B are attracted to each other, χ is less than 0; when A and B repulse each other, χ is greater than 0. As can be easily seen in **Fig. 2**, when $\chi < 2$, f_0 only has one minimum; when $\chi > 2$, f_0 has two minima and one maximum. A bifurcation takes place when $\chi = 2$, which essentially alters the free energy density.

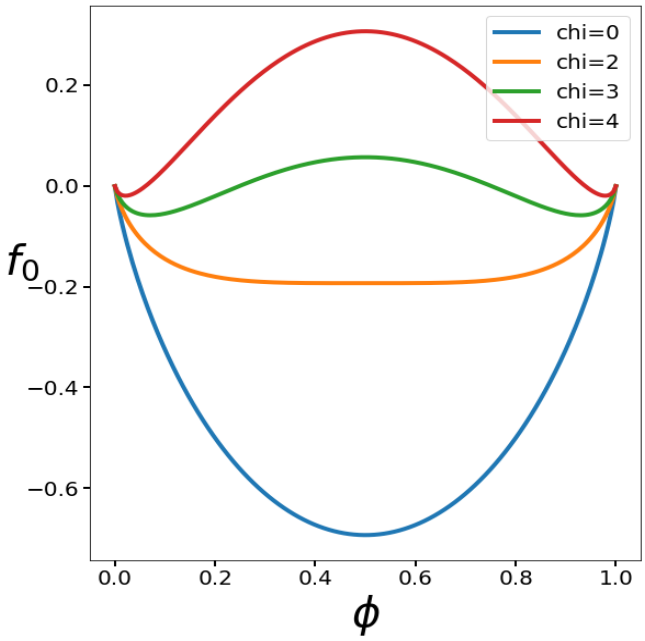

Figure. 2: Plot of the symmetric part of free energy density at various values of χ

For better illustration, we scrutinized two typical cases, χ = 0 and χ = 4. **Fig. 3** shows the free energy density for the mixed state in blue solid lines and the separated state in green dotted line. As can be seen in **Fig. 3**, when χ = 0, for any initial concentration represented by ϕ_0, the system always requires extra free energy to demix into any two separate states ϕ_1 and ϕ_2, where the green dotted line is higher than any point on the blue solid line between ϕ_1 and ϕ_2; when χ=4, there exists a range of ϕ_0 to separate into two demixed compositions ϕ_1 and ϕ_2, where the green dotted line is lower than any point on the blue solid line between ϕ_1 and ϕ_2. This is the situation where phase separation can happen spontaneously.

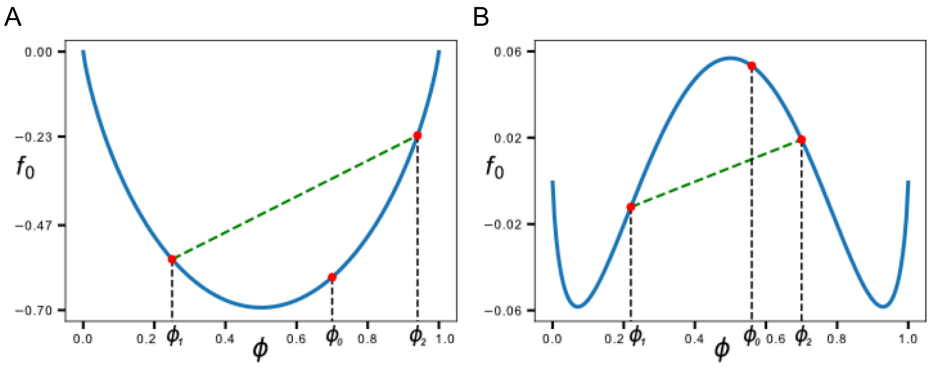

Figure. 3: The blue solid line and the green dotted line represent the free energy density for the mixed state and separated state, respectively. (A) $\chi = 0$. The green dotted line is always higher than the blue solid line, indicating an extra energy requirement for separation; (B) $\chi = 4$. The green dotted line is below the blue solid line, making spontaneous phase separation possible.

To be more precise, we can specify the conditions under which separation can happen. According to fundamental work on liquid-liquid phase separation, when $d^2f/d\phi^2 < 0$, any local perturbation will result in spontaneous separation. Such a formation is named **spinodal decomposition**. When $d^2f/d\phi^2 > 0$ and between the two minima, only sufficiently large global perturbations can make phase separation happen. Such an approach is called **nucleation**. Their boundary is named **spinodal line**. Now, if the free energy density function is symmetric, when ϕ lies outside the two minima, phase separation cannot happen. The boundary determining whether phase separation can take place or not is called **binodal line**.

Based on the criteria above, we plotted the phase diagram of a binary mixture. In fig. 4, we represent the initial concentration by ϕ in the x-axis and vary χ in the y-axis. The region confined by the spinodal line is the **unstable region**, in which separation can take place under any local perturbation. By contrast, the region between the binodal line and the spinodal line is the **metastable region**, where only sufficiently large global perturbations can initiate separation.

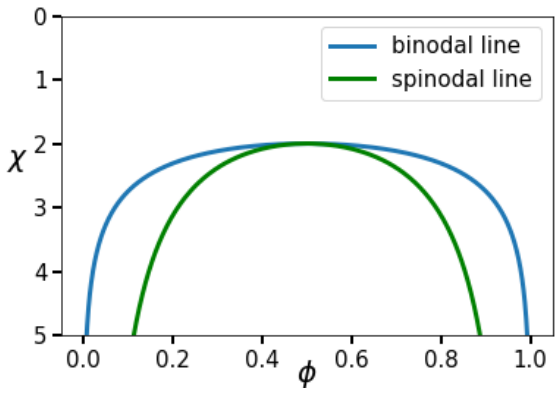

Figure. 4: Binary phase diagram. The binodal line shows the boundary between conditions

under which phases can and cannot separate. The spinodal line shows the boundary between two different formations: spinodal decomposition and nucleation. The area confined by spinodal line is the unstable region while the area between the bimodal line and spinodal line is the metastable region.

As mentioned above, our system is a ternary mixture system consisting of two multivalent proteins and water, which is a bit more complicated. To capture the basic features of three-component phase separation, we used a similar theoretical model for simulation. The free energy density f is now written in the unit of k_BT as:

$$f = \phi_1 \ln \phi_1 + \phi_2 \ln \phi_2 + \phi_3 \ln \phi_3 + \chi_{1-2}\phi_1\phi_2 + \chi_{1-3}\phi_1\phi_3 + \chi_{2-3}\phi_2\phi_3 + \frac{\lambda_1}{2}|\nabla\phi_1|^2 + \frac{\lambda_2}{2}|\nabla\phi_2|^2 + \frac{\lambda_3}{2}|\nabla\phi_3|^2,$$

where ϕ_1 denotes the first multivalent protein (or example FKBP f), ϕ_2 denotes the second multivalent protein (for example Frb) and ϕ_3 denotes water. An intrinsic relation of the three is given by:

$$\phi_1 + \phi_2 + \phi_3 = 1$$

Phenomenologically speaking, ϕ_1 and ϕ_2 condensate together and separate from ϕ_3. For computational convenience, χ_{1-2} and χ_{1-3} are assumed to have values above 2 and χ_{2-3} below 2. A ternary phase diagram is calculated in a similar way by determining whether ϕ_1 and ϕ_3 separate and whether ϕ_2 and ϕ_3 separate. The results are shown in figure 5.

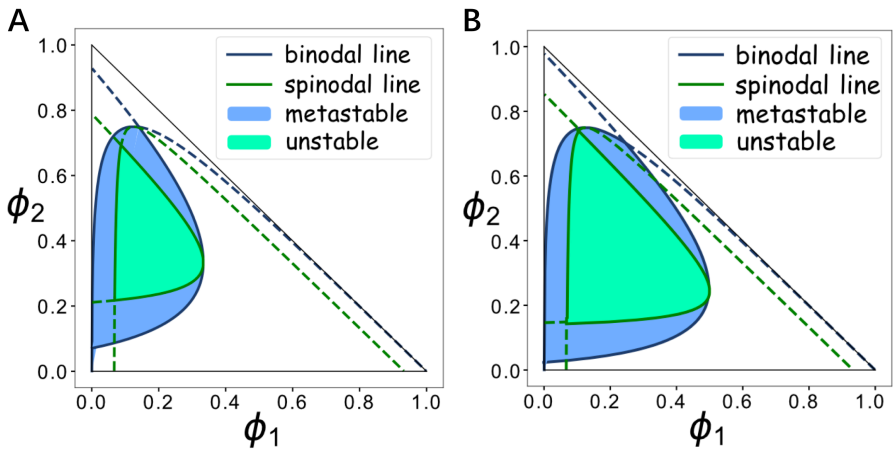

Figure. 5: Ternary phase diagrams. (A) $\chi_{1-2} = 0$; $\chi_{1-3} = 8$; $\chi_{2-3} = 3$; (B) $\chi_{1-2} = 0$; $\chi_{1-3} = 8$; $\chi_{2-3} = 4$.

The phase diagram only provides a rough approximation of where phase separation can happen; it is insufficient to predict what happens after the separation. Hence, we further recur to the continuum model first proposed by Cahn and Hilliard to simulate a dynamic process.

$$\frac{\partial c}{\partial t} = \nabla \cdot (M \nabla \mu)$$

$$\mu = \frac{df}{dc} - \lambda \nabla^2 c$$

We used the finite element method in a 100×100 mesh and selected the Neumann boundary condition to solve the partial differential equations above. The Crank-Nicolson method was used for time-stepping with a footstep of 2.0×10^{-3}. The initial composition is given by adding a perturbation of strength 10^{-2} to a homogenous sate. A typical result is given as follows:

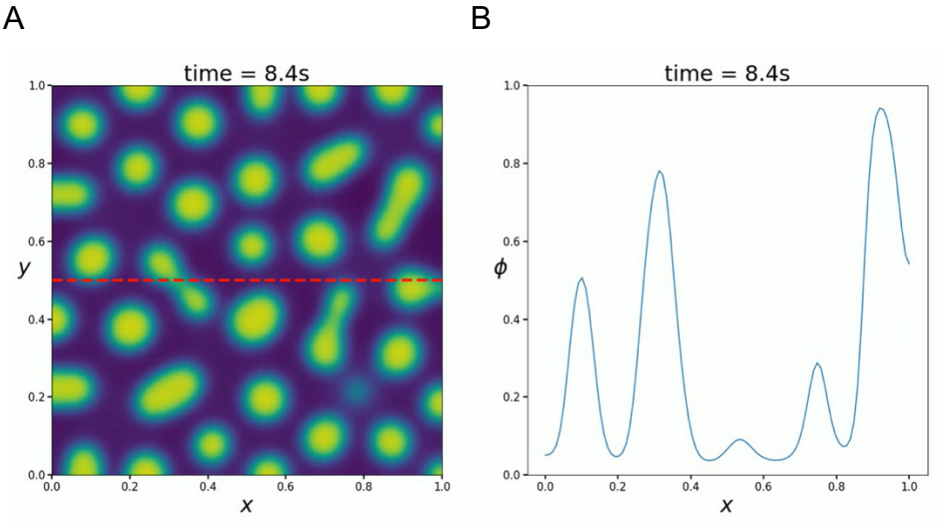

Figure. 6: Simulation for dynamic evolution of phase separation under χ_{1-2} = 0, χ_{1-3} = 3, χ_{2-3} = 4. (A) The concentration distribution of ϕ_1; (B) The centration of ϕ_1 on the sampled red dotted line in (A).

We further adjusted the interaction strength between the two proteins, thus affecting both χ_{1-3} and χ_{2-3}. As χ increases, indicating a stronger interaction, the time for phase separation to occur is decreased, which is in accordance with our experimental results.

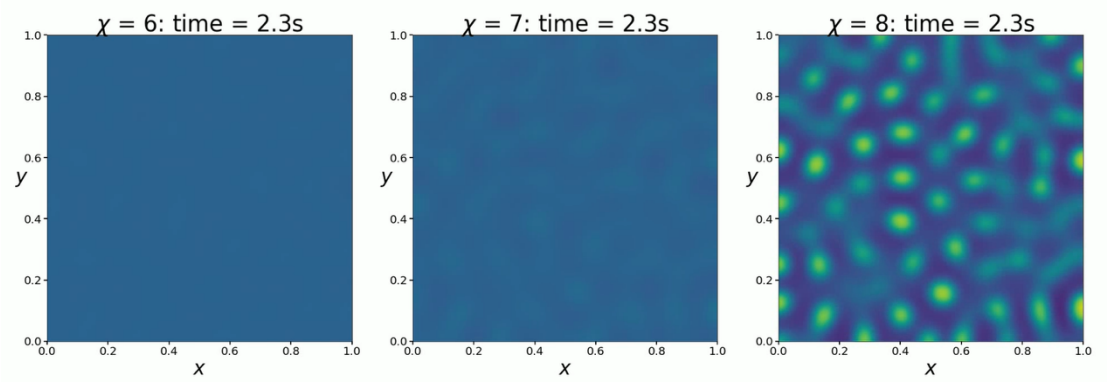

Figure. 7: Simulation of phase separation under different interaction strengths. The stronger the interaction, the faster the separation emerges.

References:

[1] Joel Berry el.al (2018). Physical principles of intracellular organization via active

and passive phase transitions

Simulation for metabolic regulation with phase separation

Before carrying out actual experiments on metabolic regulation, we conducted several computational simulations.

First, a conceptual model was established. To simplify the model, we capture the basic features of phase separation as compartments. We assumed that there are two boxes with equal volumes, one with dichotomous separate composition and the other with a uniform mixture. They are shown in Fig. 1 to represent the situations with and without phase separation, respectively. In this instant, the total amount of enzyme and substrate are identical in both boxes. The difference is that enzyme and substrate are distributed homogeneously in the uniform mixture, while they are divided into two parts in the separated case. The volumes of the two parts are denoted by χV and (1-χ)V, which add up to V, which is the total volume for both boxes. The enzyme is condensed in the χV part, and we assumed that its concentration is enhanced by p. The enzyme concentration is then written as $p[E]_0$. To guarantee that the total amount of enzyme remains unchanged, the enzyme concentration in the other part is automatically $\frac{1-p\chi}{1-\chi}[E]_0$. The substrate is treated in the same way: q[S] in the χV part and $\frac{1-q\chi}{1-\chi}[S]$ in the (1-χ)V part. For convenience, we stress here that p is assumed to be a number larger than one in all subsequent cases, but there is no limit on q.

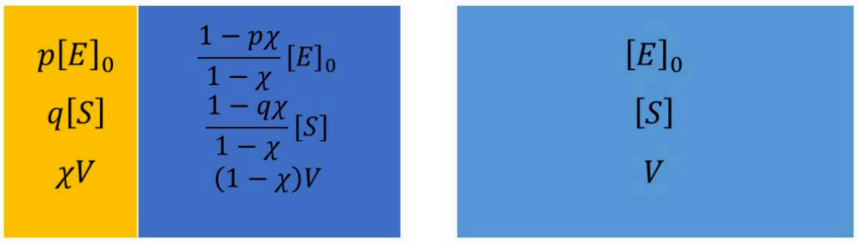

Figure. 1: Illustration of a dichotomous separate box and a uniform box.

Next, we coupled them with a typical enzyme kinetic reaction model shown in Fig. 2. Considering a quasi-steady-state and the conservation of enzyme, the instantaneous reaction rate can be expressed using the Hill equation:

$$v_0 = \frac{k_{cat}[E]_{tot}[S]^n}{K_M + [S]^n} = \frac{k_{cat}[E]_{tot}}{1 + \left(\frac{K_A}{[S]}\right)^n} \qquad (1)$$

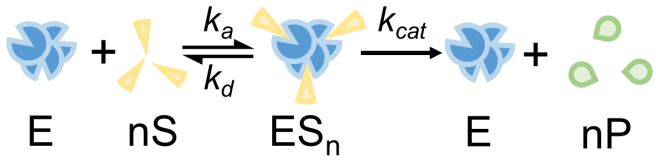

Figure. 2: Mathematical representation of typical enzymatic kinetic reaction.

Thus, the instantaneous amounts of product in the two cases are:

$$\mathrm{Q}_{separation+} = \frac{k_{cat} p [E]_0 \chi V}{1 + \left(\frac{K_A}{q[S]}\right)^n} + \frac{k_{cat} \frac{1 - p\chi}{1 - \chi} [E]_0 (1 - \chi) V}{1 + \left(\frac{K_A}{\frac{1 - q\chi}{1 - \chi}[S]}\right)^n} \qquad (2)$$

$$\mathrm{Q}_{\mathrm{separation}-} = \frac{k_{cat} [E]_0 V}{1 + \left(\frac{K_A}{[S]}\right)^n} \qquad (3)$$

To see the effect of how separation affects reaction rate, we take the quotient of the two and define it as $\tilde{Q}$:

$$\tilde{Q} = \frac{Q_{separation+}}{Q_{separation-}} = \frac{p\chi \left(1 + \left(\frac{[S]}{K_A}\right)^{-n}\right)}{1 + \left(q \frac{[S]}{K_A}\right)^{-n}} + \frac{(1 - p\chi)\left(1 + \left(\frac{[S]}{K_A}\right)^{-n}\right)}{1 + \left(\frac{1 - q\chi}{1 - \chi} \frac{[S]}{K_A}\right)^{-n}} \qquad (4)$$

Then if $\tilde{Q} > 1$, separation accelerates reaction; if $\tilde{Q} < 1$, separation decelerates reaction.

It can easily be seen that the effect of enzyme concentration is nearly linear. Thus, even when the enzyme condenses, if the substrate still remains uniformly distributed, i.e. p > 1 and q = 1, it has no effect on the reaction rate. In other words, $\tilde{Q}$ = 1 once q = 1. To conclude, if we aim to alter the reaction rate through phase separation, a heterogeneous distribution of substrate must be satisfied.

From another perspective, we can regard equation (4) as a relation between the dependent variable $\tilde{Q}$ and the independent variable $[S]/K_A$ under parameters p, q and χ. Here are some typical calculation results:

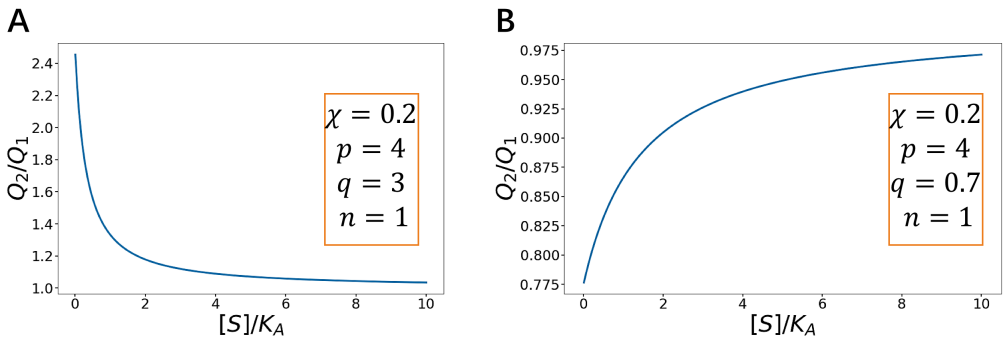

Figure. 3: (A) $\mathrm{p} > 1,\ \mathrm{q} > 1$. The reaction is significantly accelerated when $[S]/K_A$ is small

while there are no apparent effects when $[S]/K_A$ is large. (B) $p > 1,\ q < 1$. Reaction is decelerated when $[S]/K_A$ is small while there are no apparent effects when $[S]/K_A$ is large

Based on the calculations, when q > 1, the enzyme and substrate condense in the same part and the reaction is accelerated; when q < 1, the enzyme and substrate condense in different regions, thus inhibiting the reaction. But in both cases, observable changes only take place when $\frac{[S]}{K_A}$ is small. The smaller $\frac{[S]}{K_A}$ is, the more obvious the changes become.

We also varied the Hill number n to see what differences will emerge. As expected, the larger n is, the more sigmoid the kinetic curve becomes, and the more significant the acceleration.

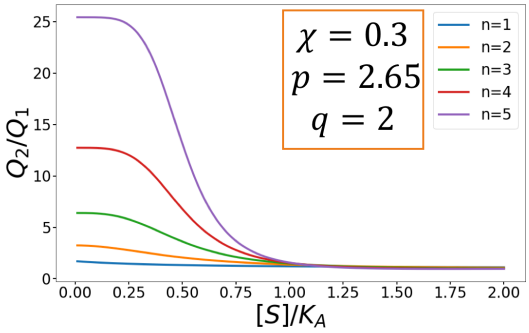

Figure. 4: Positive cooperative binding promotes the acceleration process.

To sum up, we arrived at several rough conclusions. For noticeable enhancement to happen, the system requires:
1. enzyme and substrate condensing in the same droplet
2. a relatively large K_M
In addition, positive cooperative binding increases the acceleration.

But how to condense the enzyme and substrate together? Since the diffusion velocity is generally larger than the reaction rate, if the substrate diffuses normally down the concentration gradient, normal distribution will almost eliminate any heterogeneous distribution of substrate instantaneously. We simulated this process by coupling reaction-diffusion equations with the previously described formula to model phase separation.

$$\frac{\partial [E]_0}{\partial t} = \nabla \cdot (M_E \nabla \mu_E)$$

$$\mu_E = \frac{df}{d[E]_0} - \lambda \nabla^2 [E]_0$$

$$\frac{\partial [S]}{\partial t} = -\frac{k_{cat}[E][S]^n}{K_M + [S]^n} + M_S \nabla^2 [S]$$

$$\frac{\partial [P]}{\partial t} = \frac{k_{cat}[E][S]^n}{K_M + [S]^n} + M_P \nabla^2 [P]$$

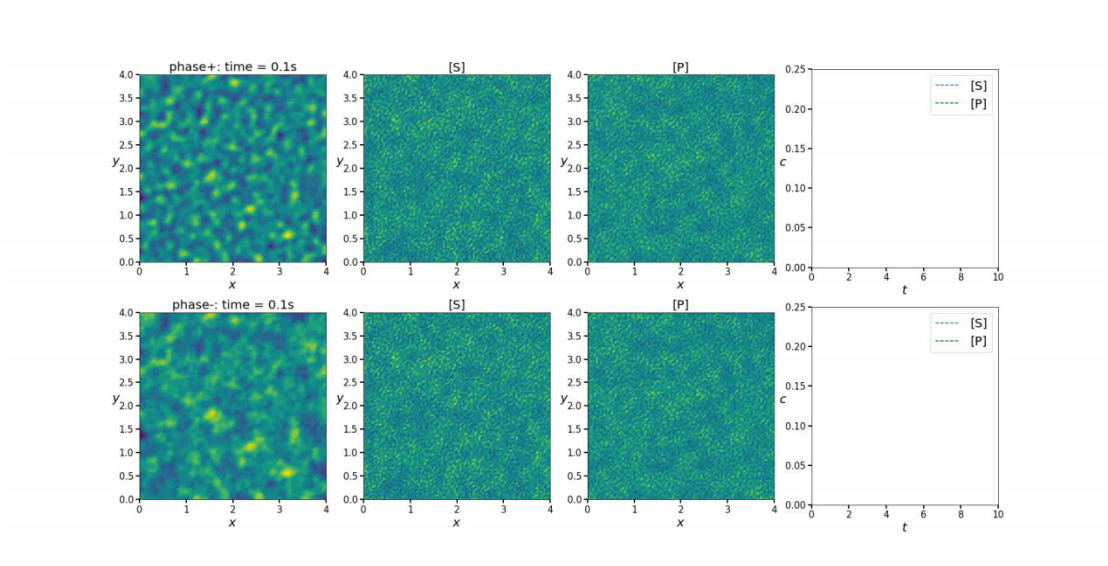

Figure. 5: Dynamic process of metabolism with and without phase separation when substrate diffuses normally down the concentration gradient. The four columns represent the concentration distribution of the enzyme, substrate, and product in a normalized plot, and the average substrate and product concentration, respectively. The upper and lower groups represent the simulations with and without phase separation, respectively.

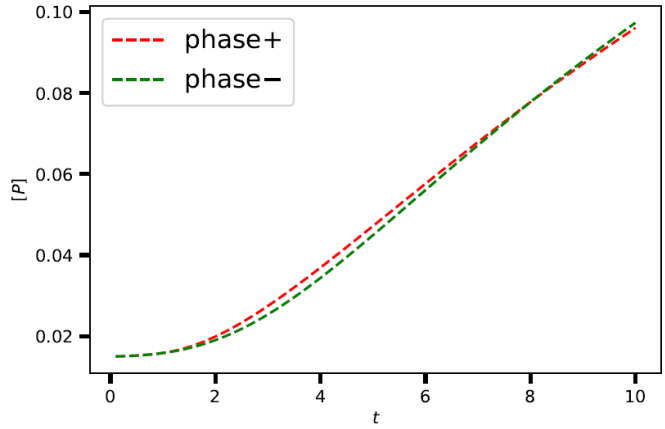

Figure. 6: The average product concentration over time. When substrate diffuses normally down the concentration gradient, the groups with and without phase separation show a slight difference.

Fortunately, if the substrate has a higher solubility in the dense oil phase, once the enzyme droplets form, the substrate can be attracted to the droplet. Hence, enzyme and droplet both condense in the same droplet. It is possible to anticipate a significant acceleration of reaction as predicted by the previous conceptual model since p > 1 and q > 1. In practical computation, the substrate is incorporated in the free energy density expression and diffuses along the chemical potential as well. The complete equations are specified as follows:

$$\frac{\partial [E]_0}{\partial t} = \nabla \cdot (M_E \nabla \mu_E)$$

$$\mu_E = \frac{df}{d[E]_0} - \lambda_E \nabla^2 [E]_0$$

$$\frac{\partial [S]}{\partial t} = -\frac{k_{cat}[E][S]^n}{K_M + [S]^n} + \nabla \cdot (M_S \nabla \mu_S)$$

$$\mu_S = \frac{df}{d[S]} - \lambda_S \nabla^2 [S]$$

$$\frac{\partial [P]}{\partial t} = \frac{k_{cat}[E][S]^n}{K_M + [S]^n} + M_P \nabla^2 [P]$$

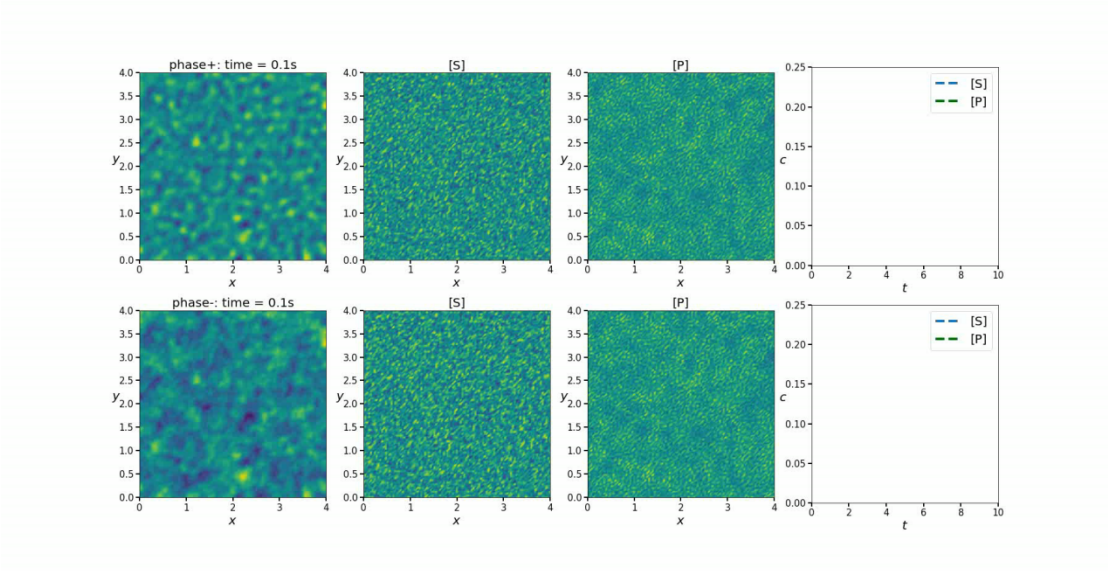

Figure. 7: Dynamic metabolic process with and without phase separation when substrate condenses together with the enzyme. The four columns represent the concentration distribution of the enzyme, substrate, and product in a normalized plot, and the average substrate and product concentration, respectively. The upper and lower groups represent the simulations with and without phase separation, respectively.

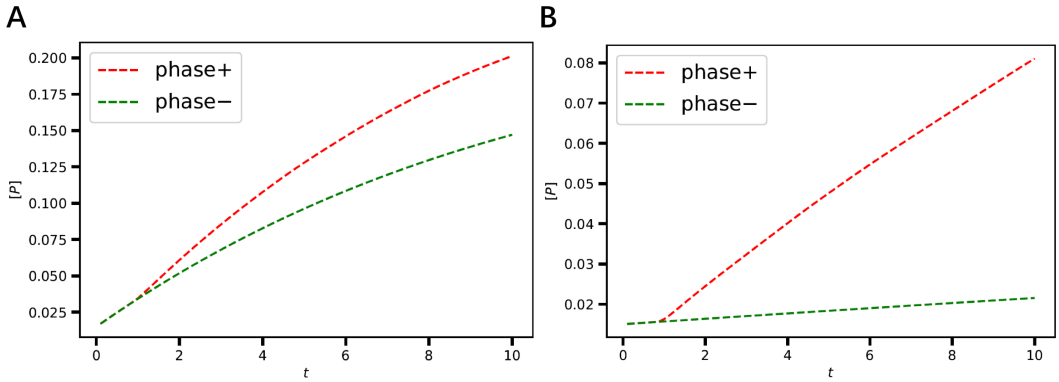

Figure. 8: The average product concentration over time. When the substrate condenses together with the enzyme, phase separation accelerates the reaction. (A) n = 1; (B) n = 4. Positive cooperative binding demonstrates a positive effect.

Judging by the simulation results, when the substrate has a higher solubility, the reaction rate is indeed increased. Incidentally, positive cooperative binding also had a positive effect in this simulation.

Generalized from the conceptual model and dynamic simulation, we were finally able to attain the two conditions for accelerating the reaction:

1. the substrate or intermediate has a higher solubility in the droplet phase
2. the reaction has a relatively large K_M